Ocean crust formation processes at very slow spreading centers: A model for the Mohns Ridge, near 72°N, based on magnetic, gravity, and seismic data

Louis Géli, Vincent Renard, Céline Rommevaux

JOURNAL OF GEOPHYSICAL RESEARCH, VOL. 99, NO. B2, PAGES 2995–3013, FEBRUARY 10, 1994

Ocean crust formation processes at very slow spreading centers: A model for the Mohns Ridge, near 72°N, based on magnetic, gravity, and seismic data

Louis Géli and Vincent Renard

IFREMER, Département des Géosciences Marines, Plouzané, France

Céline Rommevaux

Institut de Physique du Globe de Paris, Laboratoire de Géodynamique, Paris, France

The Mohns Ridge, in the Norwegian Greenland Sea, is one of the slowest spreading centers of the mid-ocean ridge system (8 mm/yr half rate). Sea Beam data acquired with R/V *Jean Charcot* near 72°N show that its rift valley floor is characterized by en échelon volcanic ridges, oriented obliquely relatively to the average strike of the ridge axis. These ridges are regularly spaced along the axis, about every 40 km, and are separated by nontransform discontinuities. Sharp positive magnetic anomalies, centered over the topographic highs, suggest that they are eruptive centers, considered as the surficial expression of active spreading cells. Over the rift valley, Bouguer anomalies obtained by subtracting the predicted effects due to seafloor topography from the measured free-air gravity field are consistent with a low density body within the lower crust having its upper surface lying at about 2 km below the sea surface. This body, if it exists, probably corresponds to the zone of low viscosity that can be inferred from the model of Chen and Morgan (1990b), which predicts the existence of a decoupling region, between the upper crust and the asthenophere below. Its width varies rapidly along-strike, from less than about 5 km to more than 15 km. In plan view, it has a pinch and swell form, which defines a series of spreading cells, the center of one cell being where the Bouguer anomaly is widest. Short wavelength (less than 10 to 20 km) along-strike variations, such as Bouguer anomaly lows centered on the topographic highs, reflect local effects associated with the presence of the eruptive centers. Seismic tomography data from a 20 x 10 km active oblique volcanic ridge near 72°22'N tend to indicate that the links between the main, low-velocity body at depth, and the magma injections centers which lie within the rift valley inner floor are probably complex.

Introduction

Specific areas of investigation for studying ocean crust formation processes are, so far, essentially located on the fast spreading East Pacific Rise and on the slow spreading Mid-Atlantic Ridge (e.g., see the review of *Detrick et al.* [1991]). Extensive studies on these areas, supported by considerable efforts in numerical modeling, have significantly contributed to the understanding of some of the fundamentals of the ridge crest thermomechanics. These studies and previous original, theoretical papers [e.g., *Sleep*, 1969; *Tapponnier and Francheteau*, 1978] have helped to understand why, and to what extent, the spreading rate and the thermal state of the asthenosphere are critical parameters controlling the ridge axial morphology and the deep crustal structure at ridge crest [e.g., *Sinton and Detrick*, 1992]. The importance of these parameters, however, cannot be fully understood without additional data covering a wide range of accreting ridges, each having different spreading rates. Very slow spreading centers, with spreading rate less than 10 mm/yr, represent a critical issue for the understanding of ocean crust formation processes, since this includes major, long portions of the mid-ocean ridge system, like, for instance, the South West Indian Ridge which extends over more than 6500 km, from the Bouvet Triple Junction, to the Rodriguez Triple Junction [e.g., *Patriat*, 1985].

To study ocean crust formation processes at very slow spreading centers, the Marine Geosciences Department of IFREMER carried out a two-cruise geophysical survey at the Mohns Ridge, in the Norwegian-Greenland Sea (Figure 1). The experiment took place during the summer of 1988 and was part of an international program including the University of Bergen and the University of Kiel. It was designed to (1) determine the scale of segmentation and (2) study the accretionary processes at the scale of one segment (Figure 2). In July 1988, a morphological study was carried out near 72°N with the Sea Beam of the R/V *Jean Charcot* over a cross-shaped survey area having a maximum lateral extension of about 250 km parallel to the ridge axis and 170 km

Paper number 93JB02966.
0148-0227/94/93JB-02966$05.00

perpendicular to it. Magnetic, gravimetric and single-channel reflection measurements were simultaneously recorded along the ship's track. From these data, the general characteristics of the ridge and the scale of the segmentation (30 to 50 km) along the axis were determined. In August 1988, a tomographic experiment was carried out with R/V *Le Suroit* to study the three-dimensional structure of a selected segment (*Lecomte* [1990]). Results of this experiment, as well as dredge data from R/V *Meteor* (C. Devey assisted by *Hirschleber et al.* [1988, p. 161-163]), and multichannel seismic data from M/V *Mobil Search* [*Roed*, 1989] and R/V *Hakon Moxby* [*Eiken*, 1991] are also used, thanks to the courtesy of C. Devey from the University of Kiel and M. Sellevoll from the University of Bergen.

THE MOHNS RIDGE

The Mohns Ridge marks the North America/Eurasia plate boundaries, between Norway and Greenland, from Jan Mayen Island up to 73°30'N, 8°E (Figure 1). It is about 580 km long and oriented in a general N60° direction. The spreading half rate, one of the slowest along the mid-ocean ridge system, averaged over the last 12 m.y. is estimated to be about 7 to 8 mm/yr. The average spreading direction, since Anomaly 7 time, is N115°, parallel to the Jan Mayen Fracture Zone (FZ) [*Vogt*, 1986]. The ridge topography consists of a series of linear, parallel flank ridges, ranging from 1000 to 2000 m deep, and a prominent rift valley, ranging from 2500 m to 3500 m deep [*Perry*, 1986]. Due to the presence of the Iceland hot spot (and also perhaps the Jan Mayen Hot Spot [*Neuman and Schilling*, 1984]), the rift valley is relatively shallow compared to the rest of the Mid-Atlantic Ridge and deepens irregularly to the northeast, from 2500 to 3000 m near the Jan Mayen FZ to 2800-3500 m near its eastern end. The Mohns Ridge is not cut by first-order offsets over its 580 km length. Instead, short, interconnected spreading axes with varying degrees of obliquity were first recognized from the bathymetry and interpreted as a "staircase" of spreading segments [*Fedhynskii et al.*, 1975]. After a careful examination of the bathymetric chart, *Vogt et al.* [1982] showed that the trace of the accreting plate boundary can actually be approximated by a series of straitghtline segments which, all together, visually fit to the axis of the rift valley. These segments range between 10 and 100 km in length along the axis and exhibit a clearly defined obliquity relatively to the global trace of the plate boundary. When viewed at the plate scale, the Mohns Ridge plate boundary thus seems to maintain an average N60° orientation by accommodating a series of separate spreading segments along its length.

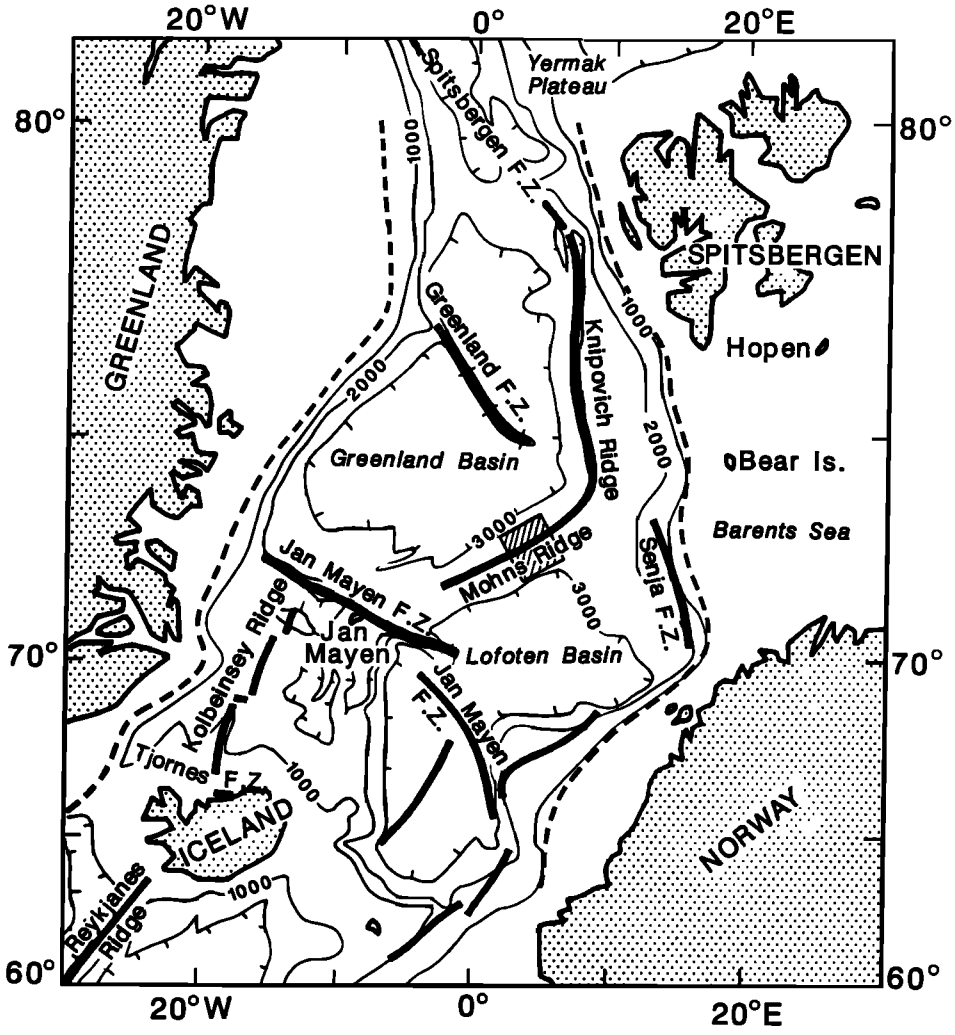

Fig. 1. Location map of the study area (within the frame), in the Norwegian-Greenland Sea.

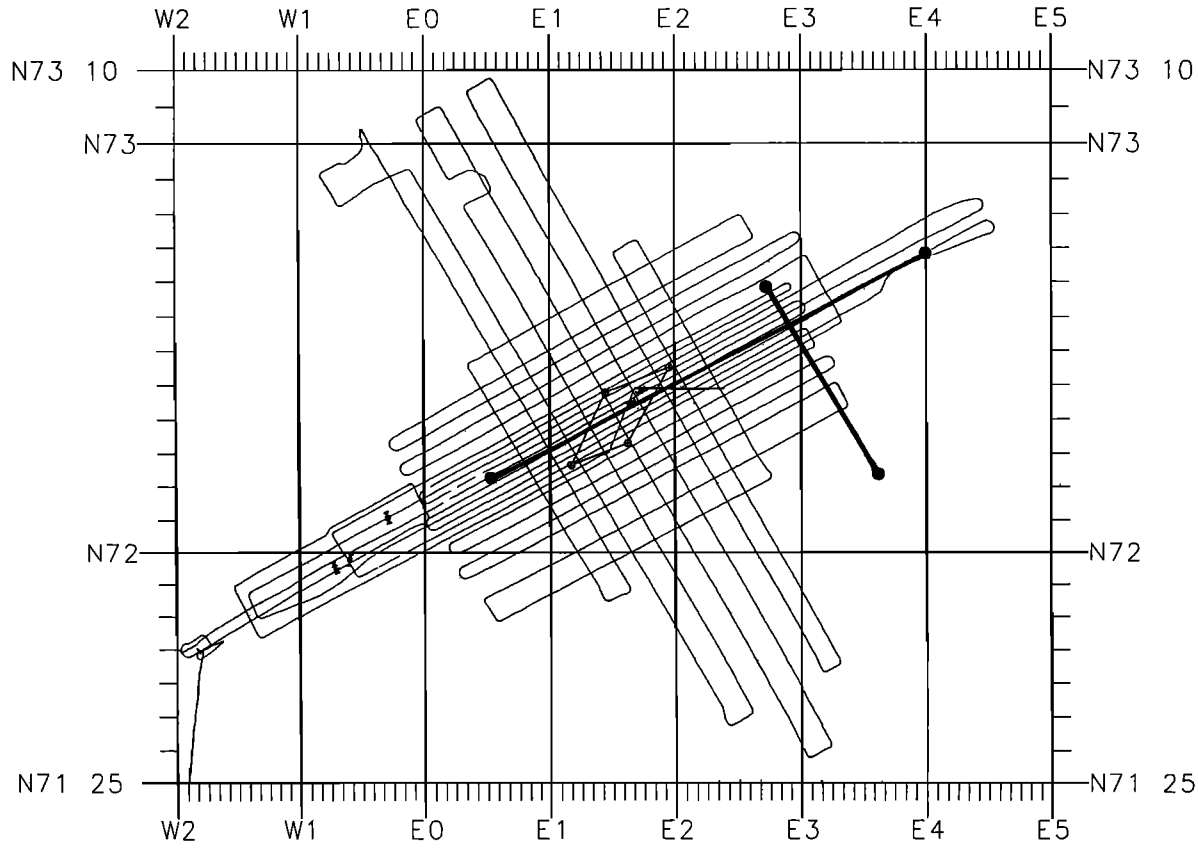

Fig. 2. Ship tracks followed by R/V *Jean Charcot* in July 1988 (Sea Beam, magnetics, gravimetrics and single channel seismics). Maps shown in Figures 3, 4, and 6 only concern the part of the explored area which is the subject of the present paper, e.g., the part where the sample density is the highest. The lozenge-shaped box is the target (shot area) for the tomographic experiment carried out with R/V *Le Suroit*. Solid dots are the corresponding Ocean bottom hydrophone (OBH) locations [*Lecomte*, 1990]. Bold lines indicate locations of dredges collected during R/V *Meteor* cruise 7-3/88 [*Hirschleber et al.*, 1988]. Thick line across the rift valley indicates ship's track during MCS profiling with M/V *Mobil Search* in April 1987. Thick line along the rift valley indicates ship's track during MCS profiling with R/V *Hakon Moxby* in September 1988.

THE SEA BEAM DATA

The Sea Beam data acquired with R/V *Jean Charcot* show that the rift valley of the Mohns Ridge near 72°N is characterized by an en échelon system of elongated topographic highs, oriented N30°, obliquely to the N60° average strike of the rise axis, which are regularly spaced, about every 40 km, and separated by nontransform discontinuities, the latter being covered by a thin blanket of sediments (Figure 3). This pattern is very similar to what has been observed on the Reykjanes Ridge, south of Iceland [*Searle and Laughton*, 1981]. Along the 150-km-long portion of the rift valley which is the subject of the present paper, a total of six highs were identified and named with letters from A to F (Table 1). The Sea Beam data clearly indicate that these highs are fissured oblique ridges (Figure 4) made of aligned volcanoes which appear to be arrayed in the N30° direction, and covered with fresh lava flows, according to dregdging results from R/V *Meteor* (C. Devey as cited by *Hirschleber et al.* [1988, p. 161-163]).

The width of the rift valley, defined as the distance from the rift walls and measured from the separation between the 2400-m contours in the average direction of plate motion, ranges between 12 and 25 km. Within the rift valley, no transform faults, but normal faults paralleling the en échelon system are documented between the different segments of the system [*Renard et al.*, 1989]. No fracture zone is observed outside the axial zone. The walls of the rift are strongly asymmetric, and stepped in an herring-bone pattern correlated with the en échelon system observed within the rift valley. On the northwestern flank, rift wall segments are very steep, reaching depths as shallow as 600 m near 72°40.5'N, 2°48'E, on the Louise Boyd Bank. On the southwestern flank, they apparently consist of a two-step staircase.

MAGNETIC DATA

The magnetic data were acquired with a Geometrics proton magnetometer, towed near the sea-surface, 300 m astern R/V *Jean Charcot*. The data (see track chart, Figure 2) were corrected using the International Reference Field (IGRF 85), but not corrected for diurnal effects (a correction was performed using a cross-over technique, but it does not change the results).

Within the rift valley, the magnetic anomaly contours reflect the en échelon pattern of the morphology (Figure 5). Sharp positive anomalies are centered over the top of the highs, from A to F. Three of the oblique volcanic ridges, C, D, and F, are characterized by very high anomaly amplitudes, in excess of 1200 nT. This argues for the existence of lava

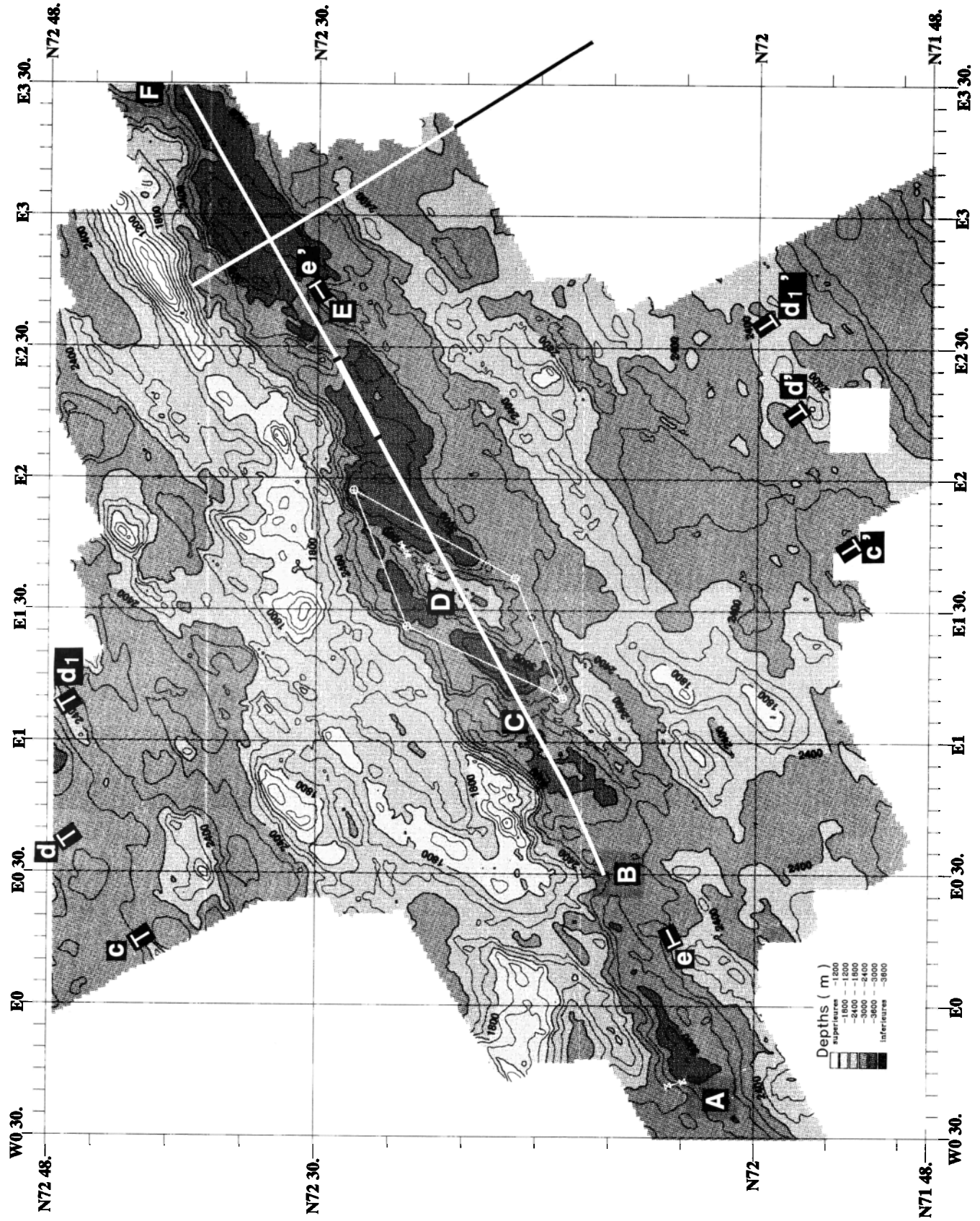
N72 48.
N72 30.
N72
N71 48.
E3 30.
E3
E2 30.
E2
E1 30.
E1
E0 30.
E0
W0 30.
A
B
C
D
E
F
e'
d1'
d'
c'
d1
d
c
e
Depths (m)
supérieures
inférieures
1200
1600
2000
2400
2800
3200
3600

TABLE 1. Nomenclature Used in the Text for Identifying the Topographic Highs That Have Been Observed Within the Rift Valley Over our Study Area

Topographic High	Latitude	Longitude	Depth, m	Maximum Amplitude of Magnetic Anomomalies, nT	Spacing, km
A	72°02'N	0°30'E	2500	800	
B	72°10'N	0°36'E	2600	600	A to B = 35
C	72°15'N	1°00'E	2800	1100	B to C = 24
D	72°22'N	1°35'E	2200	1400	C to D = 16
E	72°30'N	2°38'E	2300	1400	from D to E = 39
F	72°42'N	3°30'E	2300	700	from E to F = 38

See Figure 3. Note that if we consider that topographic highs C and D are associated with the same spreading cell at depth, the average spacing between the different cells range between 35 and 40 km.

injection centers: ridge volcanism is taking place on the topographic highs. These oblique, volcanic ridges within the rift valley are interpreted as the surficial expression of active spreading cells [*Renard et al.*, 1989]. The en échelon system within the rift valley, the steplike morphology of the rift walls, and the magnetic anomaly pattern suggest that seafloor spreading takes place perpendicularly to these ridges, and not perpendicularly to average strike of the Mohns Ridge axis: in that sense, the term "oblique spreading" is actually inappropriate at the scale of the spreading cell. At the plate scale, however, seafloor spreading is actually oblique, and the plate motion is parallel to the strike of the Jan Mayen fracture zone, as proposed by, e.g., in the N115° to N120° direction which is consistent with other proposed flow line orientation [*Vogt*, 1986].

MODELING THE MAGNETIC DATA

As a result of this process of "nucleated and oblique seafloor spreading" that we describe here, the pattern of magnetic anomalies is complex and difficult to interpret. The data lines cannot be simply modeled with methods commonly used to identify the magnetic polarity reversals boundaries [e.g., *Heirtzler and Le Pichon*, 1965]. An attempt [*Géli*, 1993] was made to identify "average" trends that appear along the N60° average direction in the pattern of magnetic anomalies. In the present paper, we show in Figure 5 the middle of the central magnetic anomaly and the middle part of Anomaly 2A (the latter was determined using an average half-spreading rate of 8 mm/yr). It appears that the magnetic anomaly highs coincide with areas where normal polarity of magnetization is predicted: with an average half-spreading rate value of 8 mm/yr, the width of the central anomaly is about 11 km, which is the approximate width of the axial magnetic anomaly highs.

In order to derive the distribution of source rocks magnetization, we performed a three-dimensional inversion of the magnetic field taking into consideration bathymetry, using the method originally developed by *Parker and Huestis* [1974], and extended to the three-dimensional case by *Macdonald et al.* [1980]. The amount of annihilator that was added to the solution was found by balancing the positive and negative magnetization on each side of the polarity boundary. In addition, as it is generally accepted, we considered that the contribution of the extrusive volcanic layer to the magnetic anomaly pattern is likely to be the most important one [e.g., *Talwani et al.*, 1971] and that this magnetized layer has a constant thickness. Given this assumption, high magnetization values derived from the inversion will mean either that the source rock magnetization is actually high or that the thickness of the magnetized layer is greater than what was initially assumed in the model. Second, we assume that with the exception of reversals, the orientation of the magnetization vector does not change within the survey area, and is consistent with a geocentric axial dipole [see *Prévot et al.*, 1979 ; *Johnson and Atwater*, 1977], but this cannot be fully justified until comparable detailed analysis has been made directly on rock samples from the Mohns Ridge.

We have considered a thickness of 500 m. Magnetization values range from -16 A/m over the rift flanks, recording crust older than the Brunhes/Matuyama boundary, up to more than 40 A/m within the rift valley, recording recent crust (Figure 6). Within the rift valley itself, there is a correspondence between the topographic highs C, D, and E and the maxima of magnetization amplitudes. Considering the model of "nucleated oblique seafloor" spreading described here, the major cause that can be invoked to explain the variations in magnetization intensity is inversion of the magnetic polarity of the rock. The magnetization highs within the rift valley actually provide indications of the Bruhnes/Matuyama reversals. The other causes such as variations in the chemical compositions of basalts, differences in grain size, and maghemitization [e.g., *Prévot et al.*, 1979] converge toward the same conclusion: the pronounced magnetization highs associated with topographic highs C, D, and E are likely to be

Fig. 3. Bathymetric map (meters) derived from gridded Sea Beam data acquired with R/V *Jean Charcot*. Grid interval is 0.5 km x 0.5 km. A, B, C, D, E, and F locate topographic highs within the rift valley (see Table 1, and explanations in text). Lines with triangles indicate locations of dredges 416/88, 430/88, and 435/88 collected during R/V *Meteor* cruise 7-3/88. Thick line along the rift valley indicates ship's track during MCS profiling with R/V *Hakon Moxby* in September 1988 (line MOH-1). Heavy segment indicates the section of the MCS record shown in Figure 14. Ticks cc', dd', d_1d_1', and ee' show the endpoints and start points of the profiles that have been seclected for the two-dimensional gravity modeling (see Figures 10 and 11).

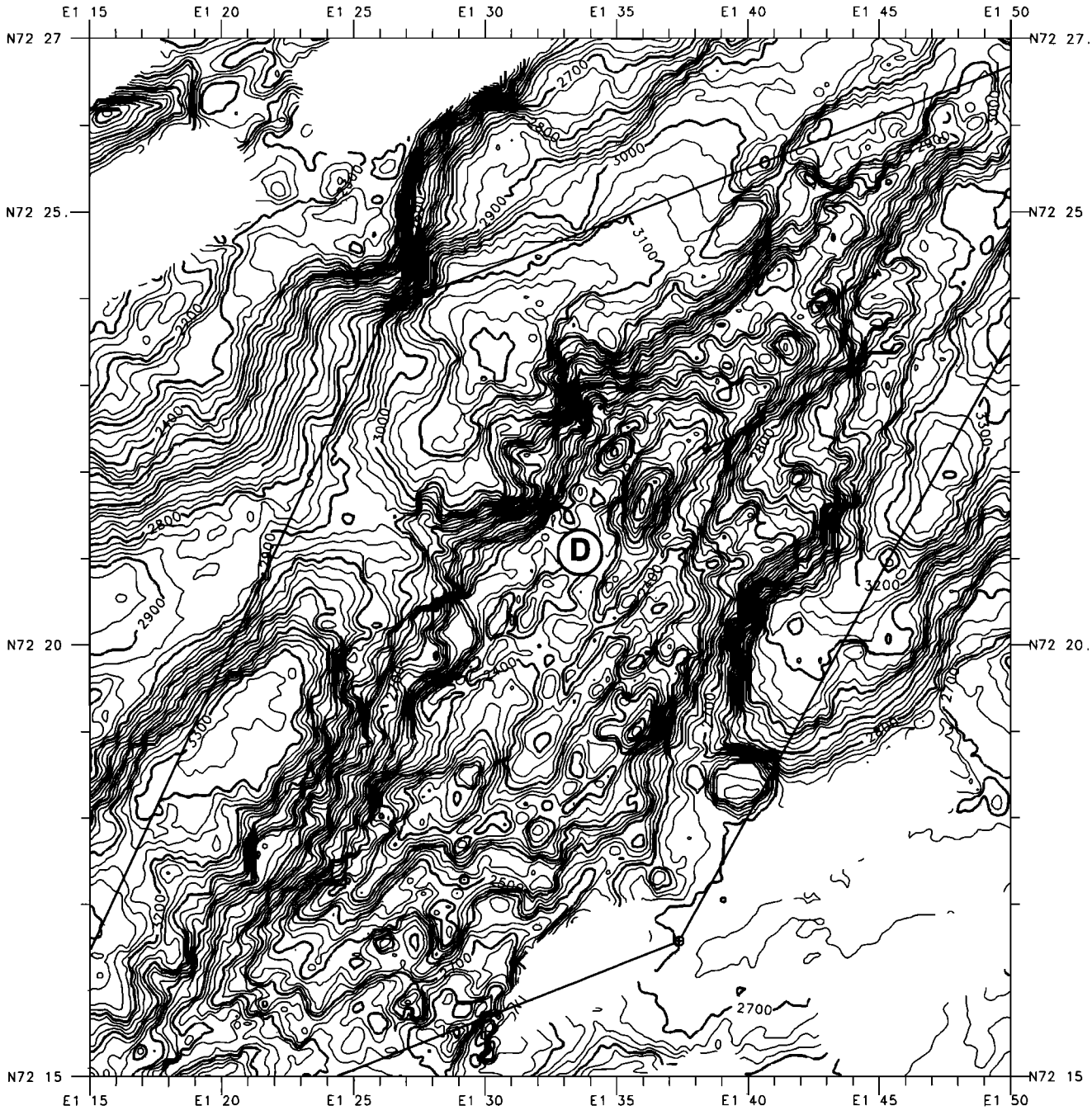

Fig. 4. Detailed Sea Beam map of topographic high D, plotted with the 25-m isobaths. The high clearly trends N30°. Note the characteristic, prominent volcano located near 72°22N, 1°36E. This volcano is very likely to be faulted and partially tectonically dismembered. At Reykjanes Ridge, similar volcanoes on oblique ridges within the rift valley were also observed with TOBI [L. Parson, personal communication, 1993]. Square gridding is used, 150 m x 150 m. Lines with triangles indicate locations of dredges 416/88, 430/88, and 435/88 collected during R/V *Meteor* cruise 7-3/88.

active magma injection centers. This contradicts the interpretation of *Dauteuil and Brun* [1993], who consider that the accretion processes actually take place within the topographic lows, like in continental rifting models.

GRAVITY DATA

The gravity data were acquired with the KSS30 BodenSee Werk gravimeter on board R/V *Jean Charcot*. The accuracy of the instrument is better than 1 mGal. Its drift, obtained by

Fig. 5. Magnetic anomalies map (nT). Data are subtracted from the International Reference Field IGRF 85 but not corrected for diurnal variations. A correction using a crossover technique has been made to correct the data from the latter effects, but it does not alter the basic results we present here. A 1 km x 1 km square grid has been used. See legend of Figure 3. Bold, solid lines indicate the trend of the central anomaly within the rift valley. Dotted, bold lines indicate the trend of Anomaly 2A.

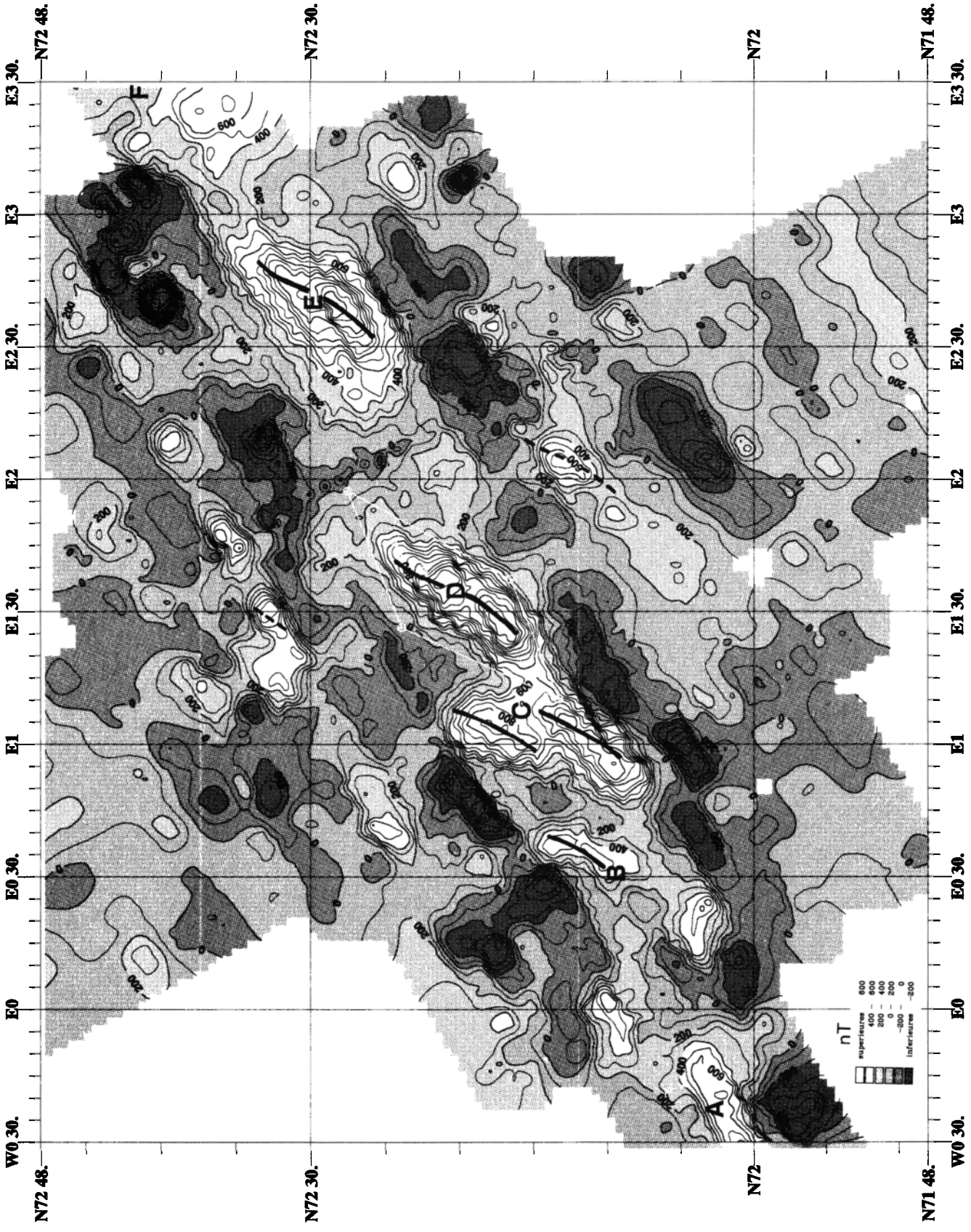
N72 48.
N72 30.
N72
N71 48.
E3 30.
E3
E2 30.
E2
E1 30.
E1
E0 30.
E0
W0 30.
A
B
C
D
E
F
nT
supérieure
inférieure

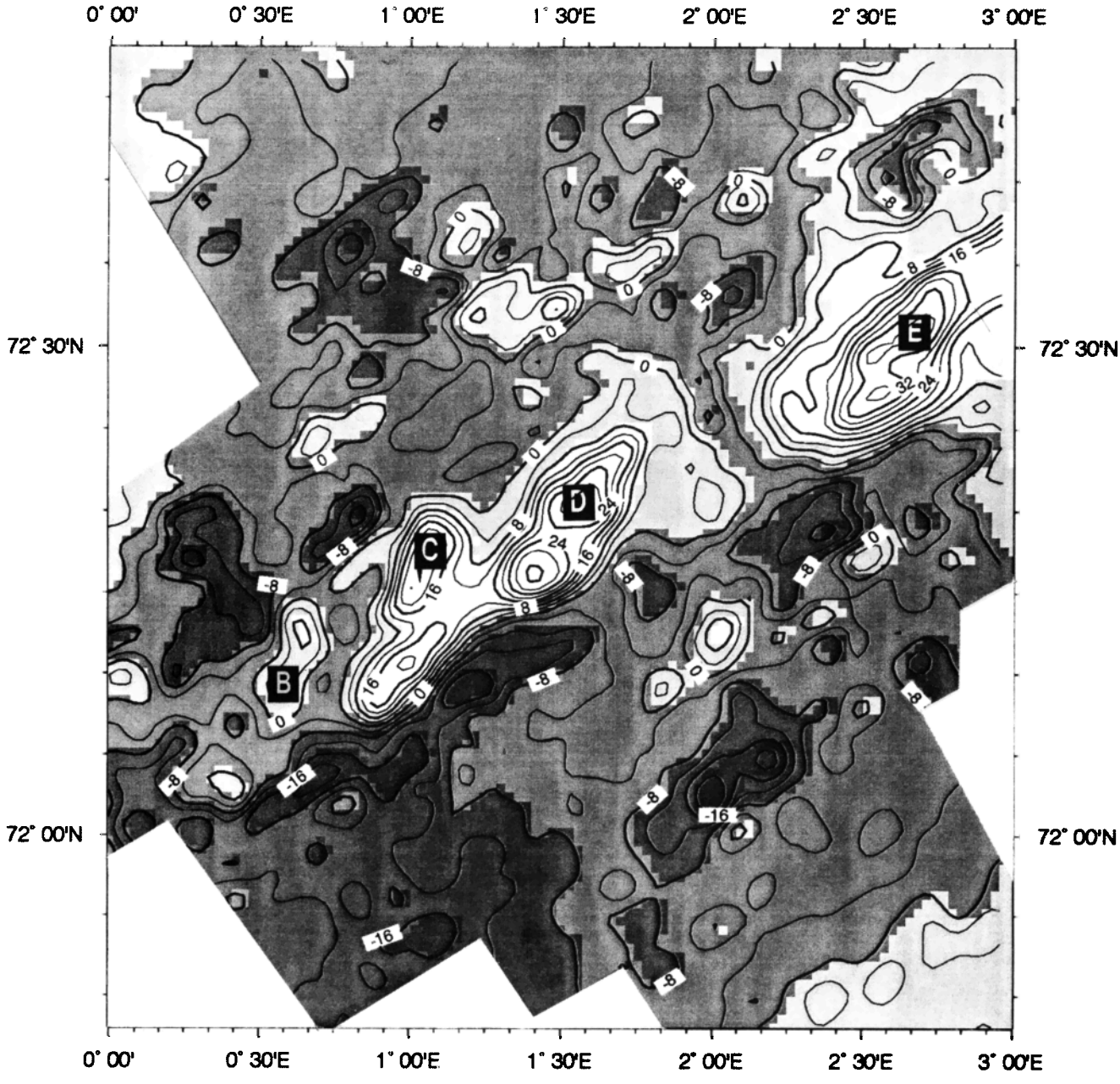

Fig. 6. Distribution of source rock magnetization (A/m). Inversion of the magnetic anomalies in presence of topography was performed using the *Parker and Huestis* [1974] method , assuming a uniform, 500 m thick, magnetized layer parallel to the seafloor. The amount of annihilator that was added to the solution was found by balancing the positive and negative magnetization on each side of the polarity boundary. See Figure 3 legend.

comparing gravity values at a reference pier in Brest before and after the cruise, is less than 2 mGal per month. Data acquired less than 5 min after course alteration were systematically excluded. A histogram of discrepancies of free-air anomalies, subtracted from the WGS 84 reference field and measured at crossing points, shows that more than 75% of the crossover error values are less than 2 mGal (Figure 7). Following the approach of *Wessel and Watts* [1988] on the accuracy of gravity measurements, we consider that crossover errors integrate all sources of uncertainty in our data set. Thus the accuracy of our gravity measurements is within 2 mGal.

Observations made in the early 1970s have shown that the Mohns Ridge has a well-defined free-air gravity anomaly pattern characterized along the rift valley by a belt of minimum values and, paralleling the rift valley on both sides, two approximately 80-100 km wide belts of maximum values in excess of 50 mGal [*Talwani and Eldholm*, 1977; *Gronlie and Talwani*, 1982]. Our results (Figure 8) concur with these observations. In addition, they provide new detail about the fine scale gravity structure near the ridge crest. Outside the rift valley, due to flank elevations, very high anomaly values are found, up to 110 mGal on the northwestern shoulder (over Louis Boyd's bank), and up to 80 mGal on the southeastern shoulder. Anomaly contours clearly correlate with bathymetry. They show a well-marked asymmetry between both flanks, and a distinct alternation between highs and lows, both along flow lines, and along isochrons. On the southeastern flank, within 50 km from the ridge axis, an en

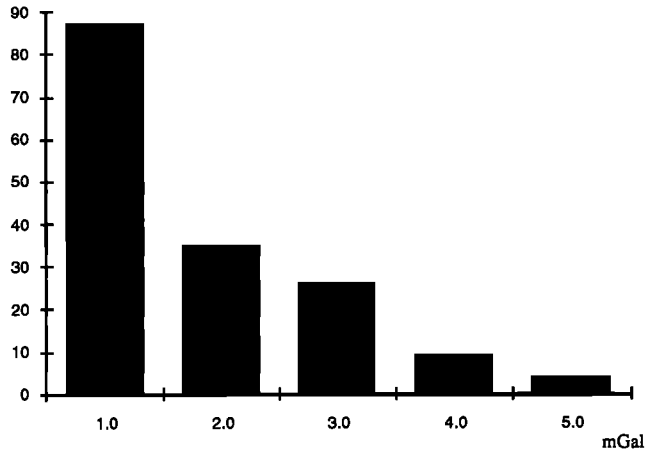

Fig. 7 : Histogram of crossover errors on free-air gravity measurements acquired with the KSS-30 on board R/V *Jean Charcot* in August 1988. A total number of 161 crossing points have been used. The cruise was considerably aided by very favorable weather and sea conditions. Navigation and positioning were performed using a Global Positioning System 8 to 12 hours a day and a LORAN-C system 24 hours a day. Maximum discrepancies of 100 m were observed between both systems. In addition, the Sea Beam information at crossing points was used for enhancing the absolute positionning accuracy, which is thus estimated to be less than 100 m.

échelon pattern is present. The rift valley is clearly defined by the 30 mGal contours. Over the rift valley inner floor, gravity lows are centered on the bathymetric lows. Near 2°E and 3°E, for instance, free-air anomalies are negative. Over the topographic saddle, C, which extends across the rift valley at 1°E 06, only a poorly defined relative gravity high is observed between two adjacent lows.

MODELING THE GRAVITY DATA

At slow spreading mid-ocean ridges, the free-air gravity anomaly signal is mostly dominated by the response to variations in the seafloor relief. We thus used direct three-dimensional modeling in order to subtract from the free-air anomaly data the predictable components of the gravity field and to produce a map which can be related directly to the subseafloor density structure (Figure 9). The gravity anomaly field due to a three-dimensional body was computed using a direct three-dimensional calculation method, based on work by *Chapman* [1979] [see *Rommevaux et al.*, this issue]. Negligible sediment cover (less than 100 m) exists within the survey area, so its contribution is ignored. Another approximation for the three-dimensional calculations is that we arbitrarily decided to ignore thermal effects due to plate cooling away from the rift axis. This option is justified by the fact that because of faulting and hydrothermal circulation within faults and cracks, it is very difficult to estimate thermal effects near the ridge crest. Almost no heat flux measurements have been performed on bare rocks, and the different laws proposed for modeling heat flux versus crustal age cannot be extrapolated to the vicinity of zero-age areas [e.g., *Parsons and Sclater*, 1977].

The effects of topography on the free-air anomaly are obtained by simply subtracting from the measured free-air gravity field the effect of an half-space of constant density bounded by the crust/water interface and a horizontal datum level, 3.5 km below the seasurface (note that this approach is slightly different from those of *Kuo and Forsyth* [1988] and *Lin et al.* [1990], who compute mantle Bouguer anomalies (MBA) by subtracting from the data the predicted effects due to a crust of constant thickness). Crustal density is set equal to 2.7 Mg m^{-3}. The average value was subtracted from the computed residuals, so as to obtain residual values having an average arbitrarily equal to zero. Resulting MBA residuals range between -25 mGal in some places of the rift valley up to more than 20 mGal over the flanks, 40 to 60 km away from the rift axis. High positive Bouguer anomaly values with wavelength greater than 50 km over the flanks are explained at the regional scale by the cooling of the lithosphere with increasing age. The rift valley is clearly delineated by the -10 isogal, while in the central part of it, variations between -10 and -25 mGal are observed. From this, we conclude that we can separate the regional components of the Bouguer anomaly field, from those which are related with accretion processes. Bouguer residuals up to -10 mGal are due to regional effects. The remaining part, between -10 and -25 mGal, reveals that local mass deficiency or local isostatic disequilibrium exists below the axis. These results support the conclusions of *Gronlie and Talwani* [1982], who modeled isostatic gravity anomalies on a two-dimensional assumption for three profiles across the Mohns Ridge and showed that the computed field matches the measured gravity field rather well, except over the rift valley, where residual anomalies of -25 to -30 mGal are present. In addition, our data show along-strike variations, such as the three lows centered on the topographic highs C, D, and E, reflecting local effects below the rift valley, at the 10 to 40 km wavelength scale.

In order to further investigate the detailed gravity structure near the ridge crest, we modeled a series of profiles perpendicular to the rift valley. For this, we used as input data the Bouguer anomalies that we derived from the three-dimensional computation, so as to remove the three-dimensional topographic effects from the data (we prefer this approach rather than to use real profiles that extend across the ridge axis because, due to the en-echelon tectonic pattern, the structure is far from two-dimensional across the ridge valley). Three pseudo-profiles were extracted from the grid of Bouguer anomalies: the first (line cc') across topographic high C; the second (line dd') across topographic high D; and the third (line $d_1d'_1$) across the axial deep, north of high D (Figure 9). These lines were modeled using the two-dimensional computation method [*Talwani et al.*, 1959] which assumes that the structure is infinitely constant along-strike. Because this method computes the effect of polyhedrons of constant density, only density structures with sharp discontinuities have been modeled. Gentle increase of density with depth, for instance, will be represented by a series of layers of constant density. "Normal" crust density is taken equal to 2.7 Mg m^{-3}, and "normal" mantle density, equal to 3.3 Mg m^{-3}. In choosing the input density structure, we assume that the numerical results of *Chen and Morgan* [1990b] for very slow spreading ridges (less than 10 mm/yr half rate) can be used for defining an acceptable starting model. Regional effects due to the cooling of the lithosphere can be modeled by assuming that a density contrast of 0.05 Mg m^{-3} exists within the upper mantle at a given interface, which corresponds to their calculated 750°C isotherm. The effect of crustal thickness on

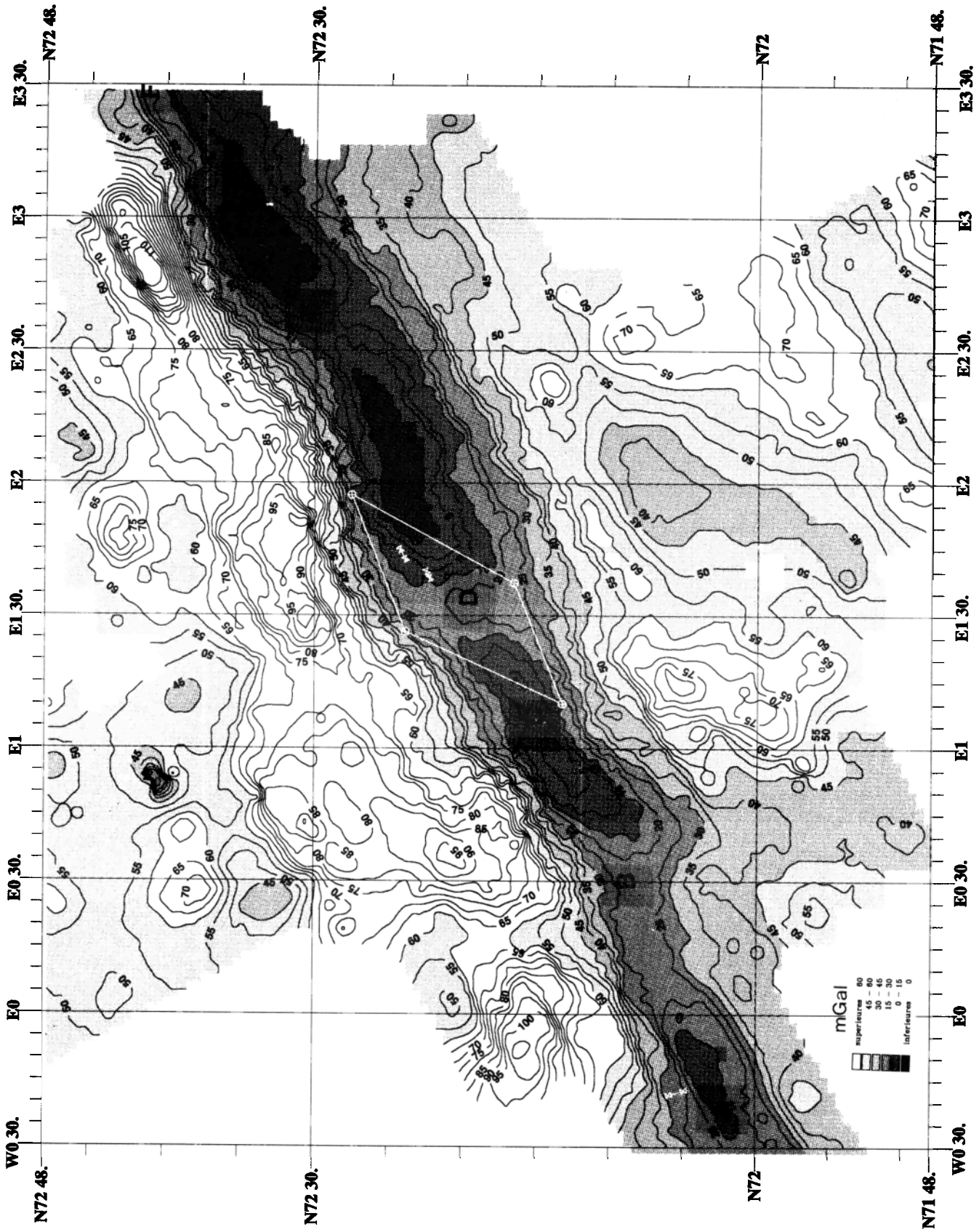
N72 48.
N72 30.
N72
N71 48.
E3 30.
E3
E2 30.
E2
E1 30.
E1
E0 30.
E0
W0 30.
mGal
supérieures
inférieures

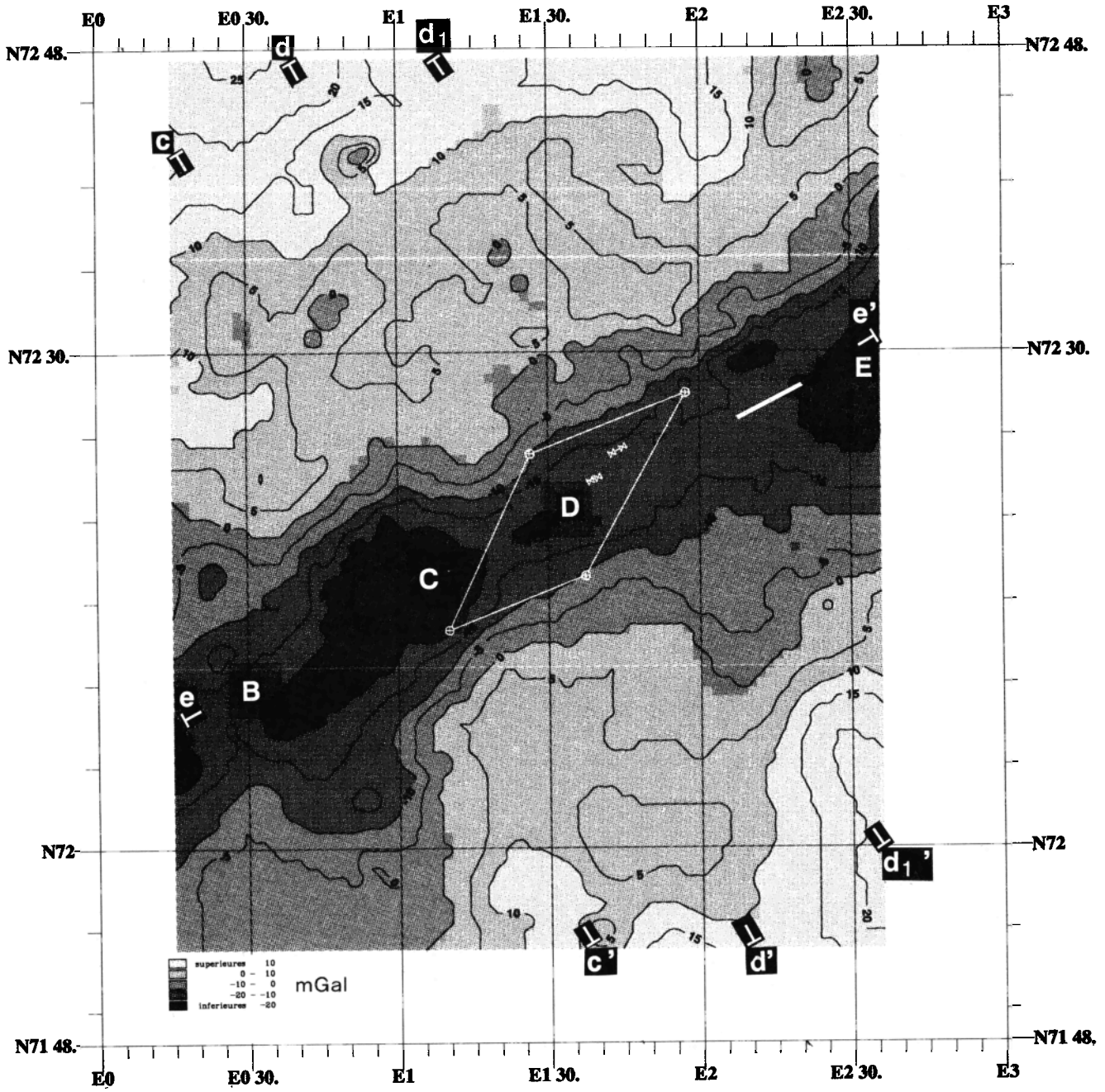

Fig. 9. Bouguer residual anomalies reduced at an arbitrary datum level, located 3.5 km below the sea surface. Lines cc', dd', d_1d_1', and ee' indicate the profiles that have been extracted for the two-dimensional modeling (see Figure 10). The direct forward modeling was performed using the method of *Chapman* [1979]: the medium is subdivided in polyhedrons, defined by a number of plane facets. The total volume integral over one polyhedron is converted to a summation of surface integrals which are analytically solved for each individual plane facet, and the result is summed for all the facets to obtain the gravity anomaly due to the total body. Between 71°52'N-72°46'N, and 0°15'E-2°36'E, where the density of measurements is highest, the bathymetric and the gravity data were gridded at a spacing of 1 km, using the cubic B spline gridding method of *Inoue* [1986]. Triangular facets were defined from points of the grid, and prisms of 100-km length were added on grid edges so as to reduce edge effects. Zero level is arbitrary. Thermal effects due to the cooling of the lithosphere have not been computed. See Figure 3 legend.

the gravity signature was studied by setting the crust/mantle interface at 6 km, 7.5 km, and 9 km respectively, below the sea surface. According to the computations of *Chen and Morgan* [1990b], these depths below sea surface correspond to crustal thicknesses h_C of about 3 km, 4.5 km, and 6 km at the ridge axis and give way to three different geometries for the computed 750°C isotherm.

For the profile across topographic high C (line cc', see Figure 10, showing results for h_C=6 km), important discrepancies of more than 8 mGal exist far off axis between

Fig. 8. Free-air gravity anomaly map (mGal). Data are subtracted from the WGS 84 reference field. A 1 km x 1 km square grid has been used. See Figure 3 legend.

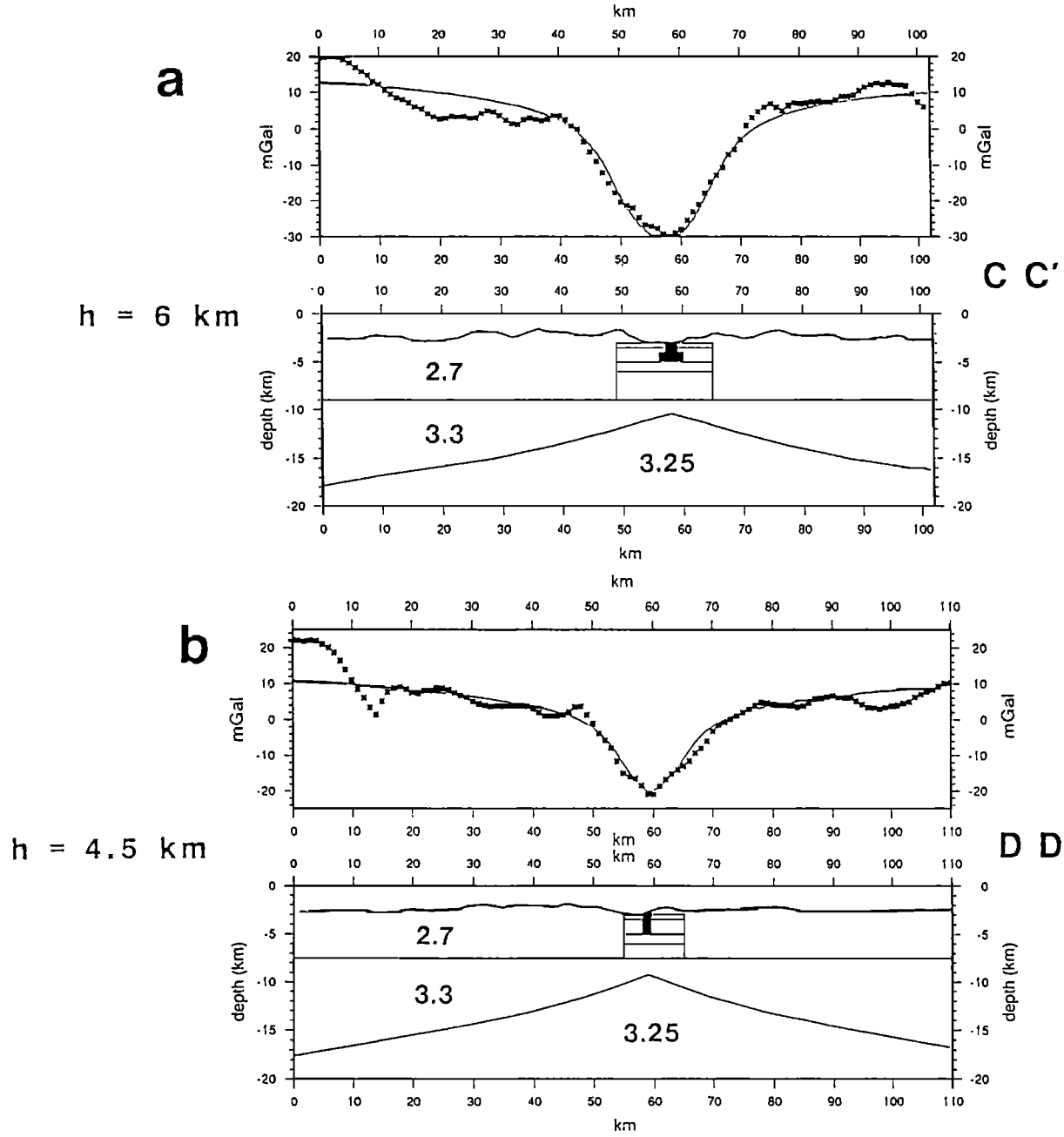

Fig. 10. Examples of two-dimensional modeling across the strike of the Mohns Ridge. The data profiles (solid squares) have been extracted from the grid of Bouguer anomalies reduced to a datum level, 3.5 km below the sea surface in order to remove the effect of topography (see Figure 9). Computations have been performed using the method of *Talwani et al.* [1959]. Zero level is arbitrary: the average value of the model has been set equal to the average value of the data. The effect due to the cooling of the lithosphere has been modeled by including a density contrast of 0.05 Mg m^{-3} at the interface defined by the isotherm 750°C. The depth of this isotherm is derived from the calculations of *Chen and Morgan* [1990b]. The modeling presented here only focuses on the area of the ridge axis. Discrepancies between the data and the model far off axis are probably due to across strike variations of crustal thickness. (a) Line cc', using a crustal thickness h_c of 6 km. The low-density body beneath the rift valley represents a layered medium, with densities ranging from 2.55 Mg m^{-3} to 2.3 Mg m^{-3}; densities in the chimney shaped body below the axis (in black) are less than 2.2 Mg m^{-3}. (b) Line dd', h_c = 4.5 km. The low-density body beneath the rift valley represents a layered medium, with densities ranging from 2.60 Mg m^{-3} to 2.40 Mg m^{-3}; densities in the chimney shaped body below the axis (in black) are less than 2.3 Mg m^{-3}. (c). Line d_1d_1', h_c = 3 km. Variations of crustal thickness must be taken into account off axis in order to fit the data; the density of the body beneath the axis is 2.5 Mg m^{-3}.

the computed field and the input data on the northwestern flank. These discrepancies are interpreted as being due to crustal thickness variations but are not considered any further in the following discussion, which focuses on what happens at the rift valley. Below the rift valley, low densitites must be introduced throughout the crust, on a 15-km-wide zone. In addition, a shallow, low-density, chimney-shaped inclusion must be introduced below the top of topographic feature C in order to account for the shorter (less than 10 km long) wavelength negative residuals ranging between -25 and -30 mGal.

For the profile across topographic high D (line dd', see

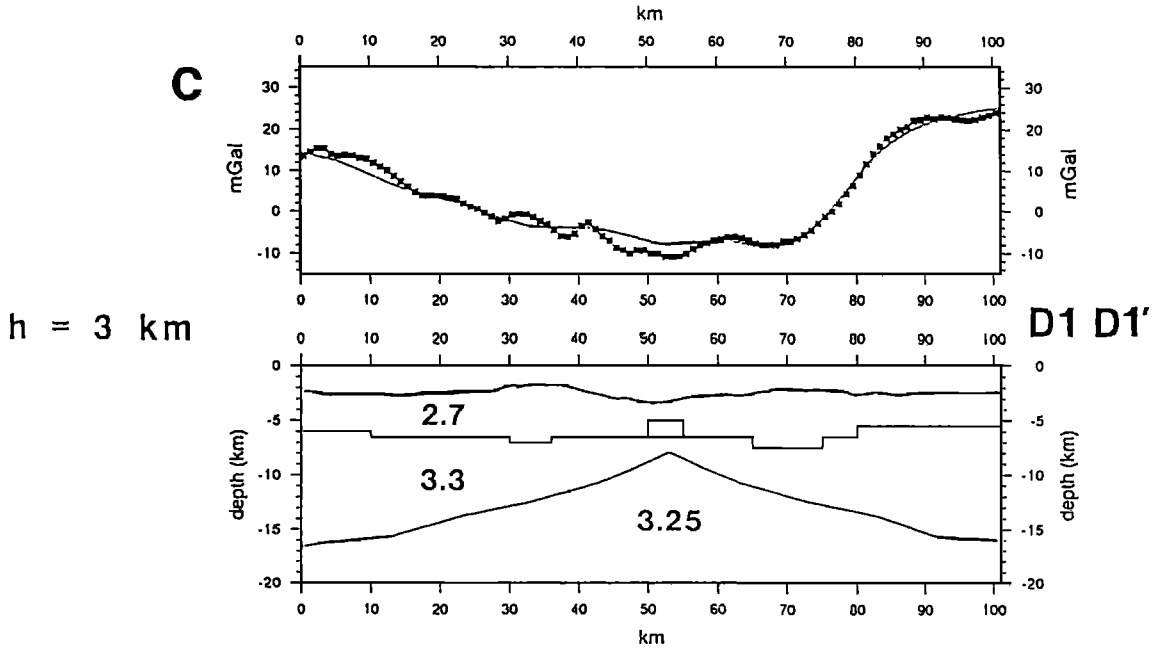

Fig. 10. (continued)

Figure 10, showing results for h_C=4.5 km), results are qualitatively very similar from those across high C. The axial zone of low densities must be only less than 10 km wide, but as in line cc', a very low-density material near the seafloor, and a low-density "chimney-shaped" body within the uppermost part of the crust must be included in order to account for the short-wavelength variations of the gravity field.

For the profile across the axial deep, north of topographic high D (line d_1d_1', see Figure 10, showing results for h_C=3 km), the gravity signal appears to be mostly dominated by off-axis variations in crustal thickness. In the axial zone, there is no need to introduce low densities in the upper crust. However, a low-density body (with across-strike lateral density contrasts of -0.20 Mg m^{-3}) is required in the deeper part of the crust, below the rift valley. The width of this body is about 5 to 10 km.

From the grid of Bouguer anomalies, we also extracted a profile lying along the central part of the rift valley (Figure 11). Along this line, the Bouguer anomalies can be explained by systematically introducing a low density chimney-shaped body below the seafloor near each topographic high, C, D, and E in order to account for the short-wavelength (<10 km) component of the Bouguer anomalies . The best fit is obtained when the maximum depth of these vertical shaped bodies is set equal to 5 km below sea surface. Below this depth, it is not necessary to introduce any longitudinal heterogeneity. This and the necessity of introducing low densities in the lower part of the crust below the axial deep along line d_1d_1' suggest that the data are consistent with the existence of a low-density, elongated, body within the lower crust all along the rise axis. This body is probably less than 2 to 4 km thick, with the top lying at about 5 km below the sea surface (that is, 1.5 to 2.5 km below the seafloor). Its width, however, strongly varies, from about 5 km along line d_1d_1', up to more than 15 km along line cc'.

DISCUSSION

Along-strike variability within the rift valley of the Mohns Ridge suggests that a three-dimensional, "oblique and nucleated", seafloor spreading process also exists at slow spreading ridges, at the 20 to 40 km long-wavelength scale. By providing additional information on the geometry of one given spreading cell and the interconnection between the deep and the surficial processes, our geophysical data set helps in understanding the ocean crust formation processes at the 10 to 40 km scale, although many questions still need to be adressed and discussed.

Existence of Eruptive Centers Within the Rift Valley

Circular-shaped, aligned volcanoes are clearly observed on the Sea Beam data from the different topographic highs lying within the rift valley. Associated with these highs, important amplitudes of the magnetic anomalies, in excess of 1200 nT in some places, do indicate the boundaries of the central magnetic anomaly. These highs also may indicate either the presence of highly magnetized rocks, or the presence of an anomalously thick layer of magnetized material, or both. In any case this implies that more basaltic rocks are being produced at these highs, which are likely to be the focii of some eruptive centers.

Source of Gravity Anomalies at Wavelength > 20 km

In August 1988 a tomographic experiment was performed to study the three-dimensional structure of topographic high D. Experimental procedure, method and results of this experiment are described in detail by *Lecomte* [1990]. Results are presented in terms of velocity anomalies relative to an initial one-dimensional model, which consists of a first order discontinuity, 3.5 km below the sea level, which separates an upper medium of constant velocity equal to 3.2 km/s, and a

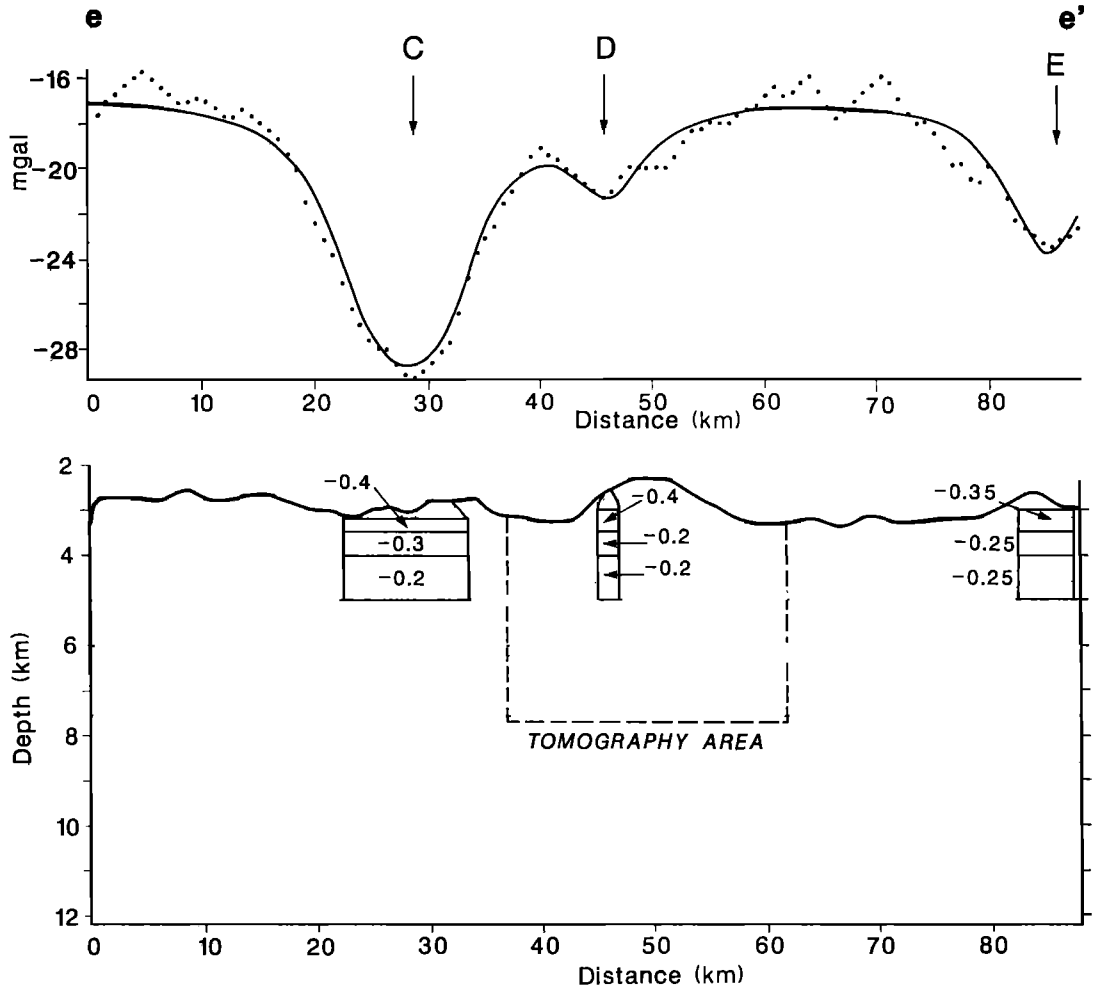

Fig. 11. Two-dimensional modeling of line ee' (see Figure 9) along the strike of the Mohns Ridge.The data profile (solid squares) has been extracted from the grid of Bouguer anomalies reduced to a datum level, 3.5 km below the sea surface in order to remove the effect of topography. Computations have been performed using the method of *Talwani et al.* [1959]. Zero level is arbitrary: the average value of the model has been set equal to the average value of the data. The frame in dashed lines indicates the location of the area of tomography.

lower medium of constant velocity gradient equal to 0.8 s^{-1} A velocity jump is set at the discontinuity, from 3.2 to 4.5 km/s immediately below the discontinuity level (Figure 12). Results indicate that velocities beneath the axial zone are lower, by about 10 to 20% than those on the sides. As shown by previous studies in other portions of the Mid-Atlantic Ridge [*Fowler and Keen*, 1979; *Whitmarsh*, 1973], differences in crustal structure exist between the rift valley area, where the crust is not completely formed, and the flank areas, where the crust is expected to be mature. There is no symmetry perpendicular to the rise axis, and a very strong heterogeneity of velocity structure is observed along the axis. Below topographic high D, within the rift valley, three horizontal cross sections are presented showing velocity anomalies at three different depth levels -3.5 km, 4.7, and 7.1 km, respectively (Figure 13). Owing to problems inherent in the technique, results for the shallowest cross section, 3.5 km depth, are difficult to analyze. On the intermediate horizontal cross section, at a 4.2-km-depth level, the velocity structure clearly defines an en échelon pattern, which delineates a N60° trend and correlates with seafloor topography at first approximation. Velocities are lower beneath volcanic ridge D than beneath the surrounding areas. The lowest velocities are encountered below the southwestern and northeastern terminations of the oblique volcanic ridge: the low-velocity areas clearly extend from the ridge to the adjacent deeps. On the deeper horizontal cross section, at a 7.1-km-depth level, isovelocity contours do not readily correlate with bathymetric contours. A distinct asymmetry is observed, east and west of the oblique ridge, the eastern part being associated with higher velocities: there is a clear shift of the low velocity area south-westward, below the adjacent deep separating topographic highs C and D. The velocity structure thus reflects a low-velocity body at depth which seems to migrate from deep intracrustal levels below the southwestern adjacent basins toward shallower levels, below the western flank of the oblique volcanic ridge.

We have seen that the gravity data were consistent with a model including a low-density body beneath the axis and within the lower crust. This body, if it exists, is less than 2 km thick, with the top lying at 5 km depth below the sea surface. It is characterized by slight density contrasts, less than 0.2Mg m^{-3}, relatively to the surrounding crust, and its width may vary considerably, from less than 10 km below C,

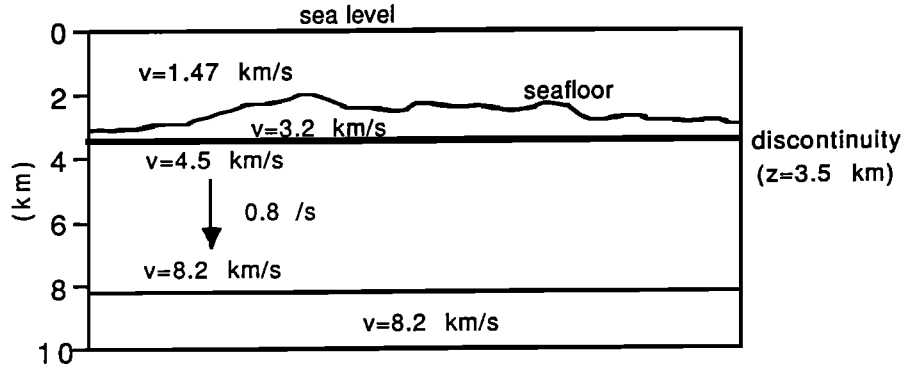

Fig. 12. Initial one-dimensional velocity model used in the inversion of the travel time data set from the tomographic experiment [after *Lecomte* , 1990].

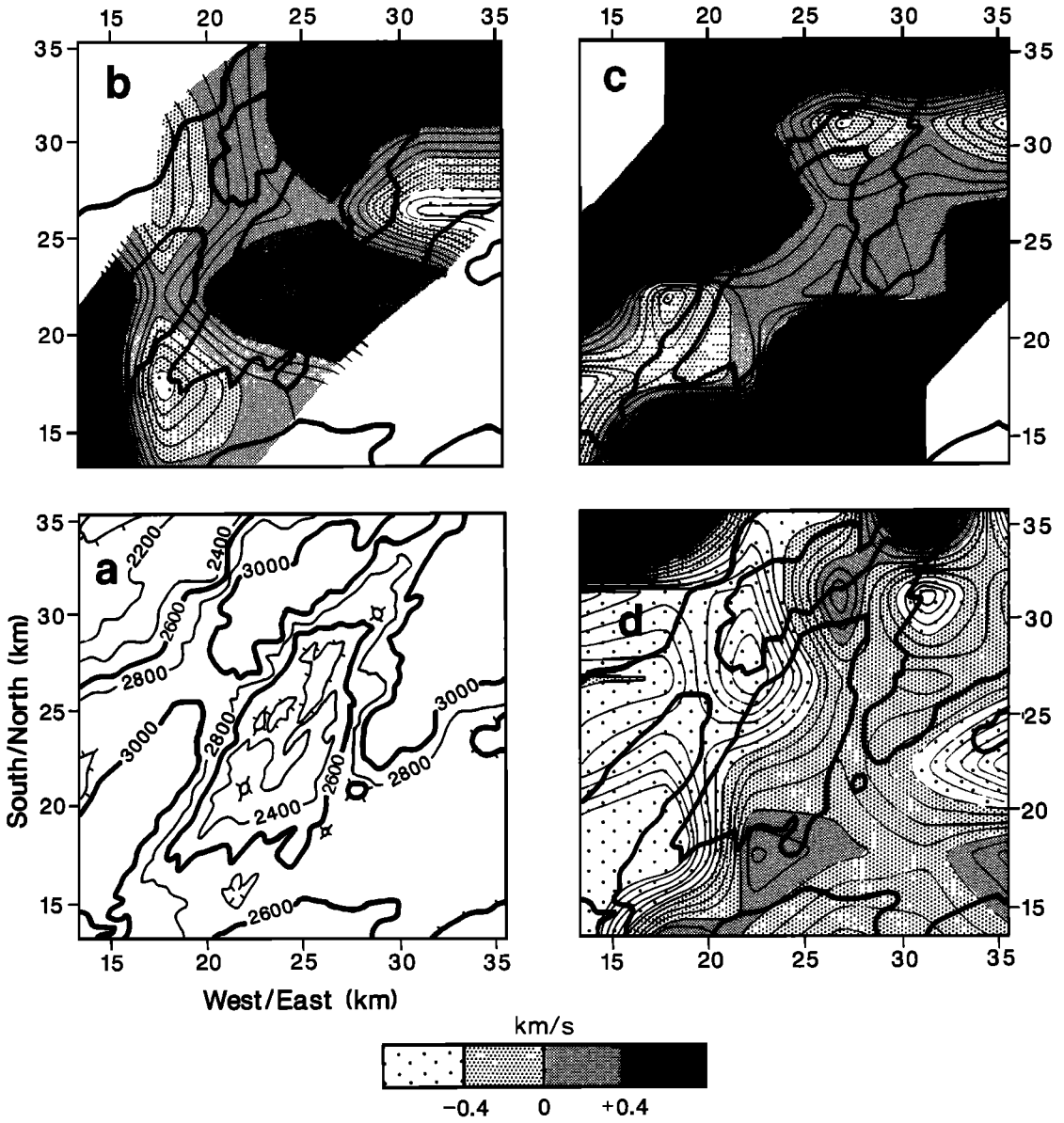

Fig. 13. Redrawn after *Lecomte* [1990]. (a) Bathymetry of the zone defined for the tomographic inversion. Horizontal sections at three different levels are displayed at (b) 3.6 km, (c) 4.7 km, and (d) 7.1 km depths. Heavy lines represent 2600 m and 3000 m isobaths. Results are given in velocity perturbations (km/s) relative to the initial one-dimensional model of Figure 12.

to more than 15 to 20 km below D. The lower crust and the upper mantle beneath the rift valley have, in plan view, a pinch and swell which apparently define a series of spreading cells, the center of each cell located where the Bouguer anomaly is at its widest. If real, this low-density body may be interpreted as the feeding reservoir from which the accreting material is supplied to the eruptive centers, and it is apparently also consistent with the one resulting from the tomographic experiment. The next question is: is there any direct evidence for a low-density body at the base of the crust ?

In April 1987, a 60-km-long multichannel reflection profile was conducted by the University of Bergen with M/V *Mobil Search* across the crest of the Mohns Ridge, on a line starting at 72°38.9'N, 2°43.4'E, and ending at 72°11.5'N, 3°39.7'E [*Olavsson et al.*, 1988; *Roed*, 1989]. Owing to the numerous side echoes and off-plane lateral reflections that appeared on the section and in absence of additional information, the data were barely interpreted. In September 1988, another 163-km-long multichannel seismic line was shot along the axis of the Mohns Ridge, also by the University of Bergen, with R/V *Hakon Moxby* [*Eiken*, 1991]. In an attempt to separate side echoes from sub-bottom reflections, *Eiken* [1991] used a simple geometrical method proposed by *Claerboutt* [1985] and concluded that some of the reflections that are observed in the seismic record also may be considered as potential candidates for subbottom reflectors. In the example given in Figure 14, one of these candidates clearly appears at about 1 s two-way travel time below the sea bottom reflection (see arrow). So far, there is no unambiguous argument concerning the reality nor the geological signification of these reflectors that our colleagues from Bergen have tentatively pointed out. We hypothetize, however, that some of them may originate at the top of a low-density body lying at depth at intracrustal levels beneath the axis of the Mohns Ridge: if, for instance, the reflector shown in Figure 14 is geologically relevant, it indicates that an interface is present at about 2 to 2.5 km below the seafloor, consistent with the depth of the top of the low-density body that we have introduced to model the gravity data.

May the Existence of a Low Velocity Body Below the Axis of a Very Slow Spreading Center Be Theoretically Supported ?

Using finite element techniques, *Chen and Morgan* [1990a, b] numerically showed that if spreading rate is equal to 10 mm/yr, and crustal thickness equal to 6 km, a region of low-viscosity material may appear within the crust, between the upper, brittle layer, and the underlying ductile upper mantle. According to these authors, this may explain why microearthquakes at the Mid-Atlantic Ridge near 23°N are clustered at depths of 6-8 km, which correspond to the Moho transition zone, and why an apparent gap in seismicity exists from 2 to 5 km depth below the rift valley axis [*Toomey et al.*, 1985]. The cluster of microearthquakes at depths of 6 to 8 km may be interpreted as an indication of the brittle failure of the uppermost mantle due to the induced viscous stresses, and the apparent gap in seismicity may correspond to the gap in the failure zone due to the low ductile flow strength of the oceanic crust. If this low-viscosity region is not at the same density as the surrounding terrain, it will migrate up and give way to eruptive centers. Hence we propose that at the Mohns Ridge: (1) the low-viscosity zone predicted by Chen and Morgan is consistent with our data set and (2) if it exists, this zone is likely to be associated with low densities.

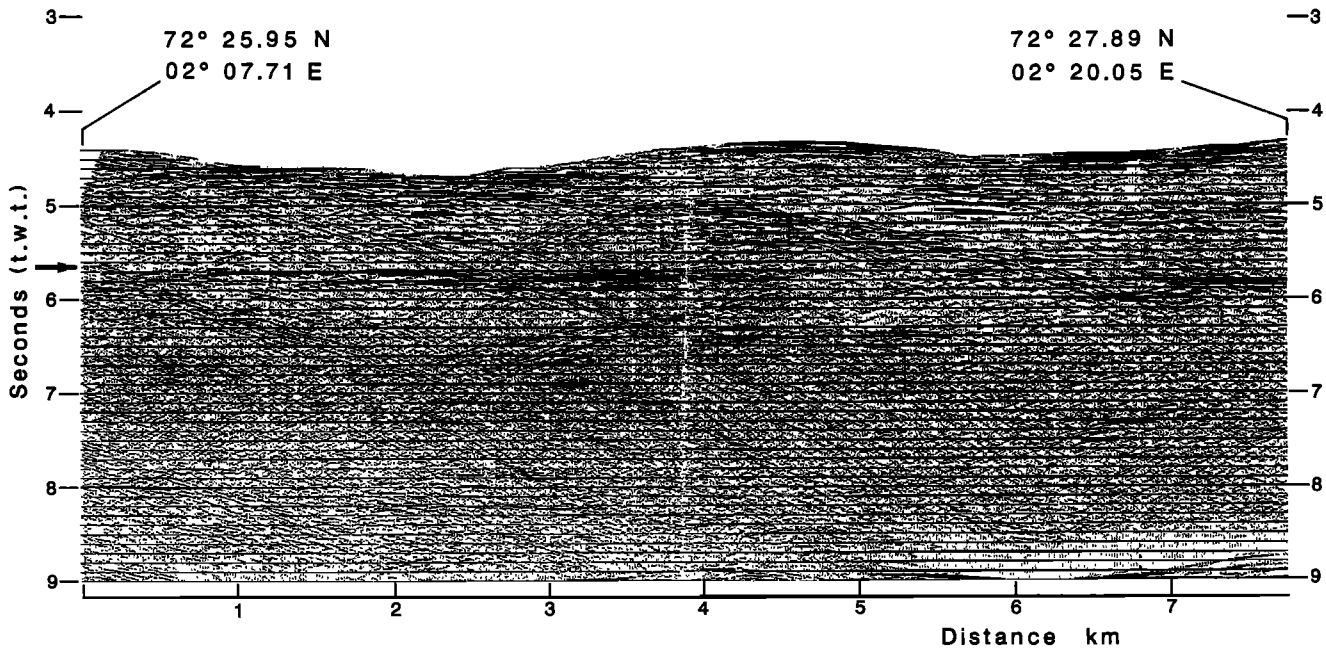

Fig. 14. Preliminary stacked multichannel reflection seismic record, acquired with R/V *Hakon Moxby* on a line shot along the rift valley, and shown by courtesy of M. Sellevoll, University of Bergen. The location of this section is indicated in Figures 2 and 3 by a heavy bold line. Some candidates for potential reflectors had been tentatively pointed out by *Eiken* [1991]. On the basis of our data set, we also think that some reflectors are probably "real", indicating the presence of discontinuous intracrustal interfaces. For instance, the reflector outlined by an arrow and located at 1 s two-way travel time (twt) after the seafloor reflection may actually indicate the top of the low-density body that we infer in our model.

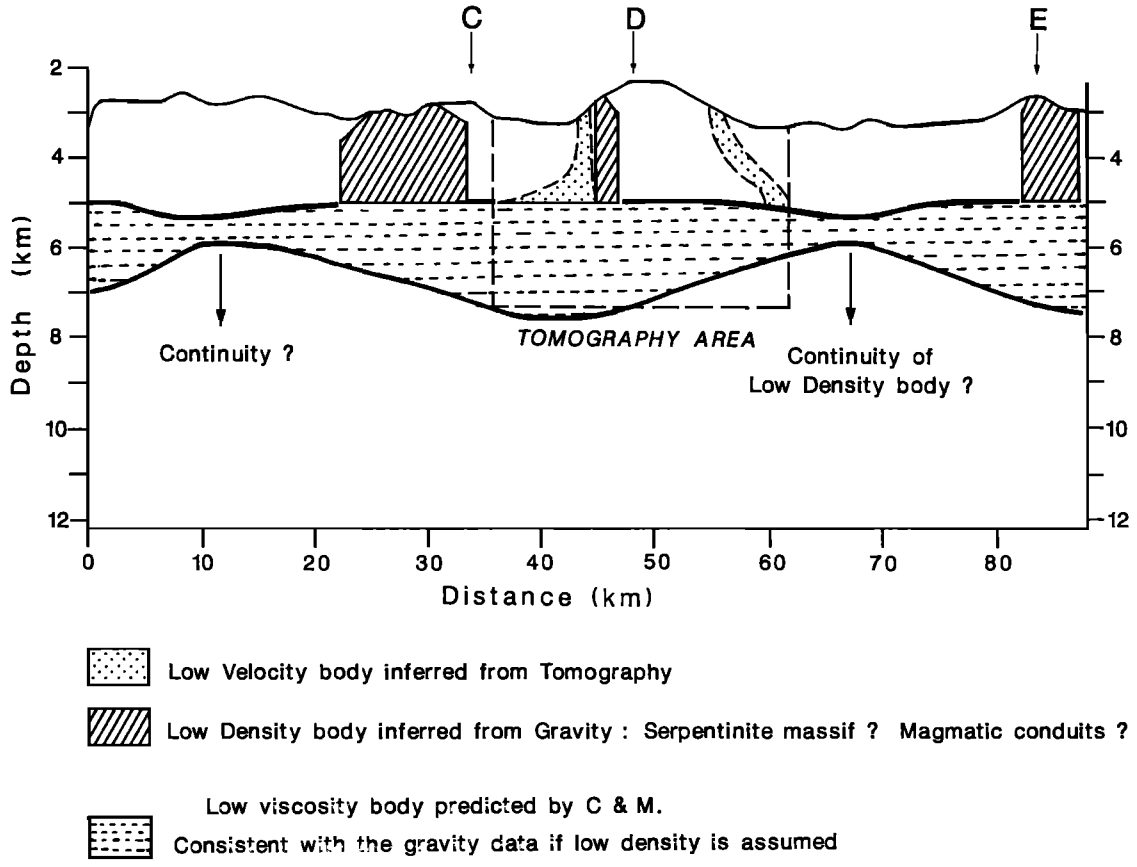

Fig. 15. Schematic section along the rift valley axis summarizing the main results of the present study. The model includes an elongated, low density body of varying width all along the rift valley, the top of this body being at about 2 km below the seafloor.

Source of Gravity Anomalies Observed Along the Rift Valley, at Wavelength <20 km

Vertical conduits, lying in the uppermost 2 km of the crust, have been introduced below the topographic highs C, D, and E in order to account for the short-wavelength (less than 10 to 15 km) variations of the Bouguer anomalies (see Figure 15). Their lengths in the direction of the ridge axis are about 10, 3, and 5 km, respectively. Their width across the axis is probaly less than 2 to 3 km. The nature of these conduits is difficult to establish on the basis of our data alone. Besides the difficulties related to the nonuniqueness of the model solutions, one problem of the gravity method is that it provides information from any direction, and not necessarily from that located below the ship. Unlike the gravity method, the tomographic method provides information from that located directly below the target area. The velocity structure below the topographic high D reflects a low-velocity body at depth which seems to migrate from below the southwestern adjacent basins upward to the western flank of the oblique volcanic ridge.

The best fitting position of the low-density conduit inferred from the gravity method below D is not exactly coincident with the position and geometry of the low-velocity zone inferred from the tomography. Merged together, the tomographic data and the gravity data, however do indicate that some links must exist between a main, 10 to 15 km wide, low-velocity body at depth and the magma injections centers which can be observed on the rift valley inner floor (Figure 15). The resolution of the indirect, geophysical methods we used does not allow us to give much finer, firmly established details. We can only conclude that the low-density, elongated region at depth provides if it exists, the major supply for the accretionnary processes that are observed within the rift valley of the Mohns Ridge, but the links between this region and the eruptive centers on the seafloor, which are probably complex, cannot be unambiguously determined.

CONCLUSION

Most of the observed morphological features we describe from the Mohns Ridge, like the segmentation along the axis and the highly variable seafloor topography near 72°N, have previously been reported from the Mid-Atlantic Ridge [e.g., *Sempéré et al.*, 1990]. Similarities between the Mohns Ridge, a very slow spreading accreting center, and the Mid-Atlantic Ridge confirm numerous other observations implying that an universal control of axial morphology probably exists at slow spreading ridges [*Schouten et al.*, 1985]. What is new, however, is that the data set we present is to date one of the most comprehensive ever acquired at the crest of a very slow spreading ridge. This data set allows us to determine the scale of the segmentation along the Mohns Ridge and provides us with some insight of the structure at the scale of one segment.

The gravity data have been explained on the basis of the physical insight provided by the model of *Chen and Morgan* [1990a, b]. Bouguer anomalies are modeled by introducing a uniform density contrast within the mantle and within the

crust, a low-density body, less than 2 to 4 km thick, is 1.5 to 2 km 1.5 to below the rift valley. This body decouples the upper, brittle part of the lithosphere, and the asthenosphere below it. Its width varies considerably along-strike, from about 5 to 10 km, up to more than 15 km in some places. We also think that some of the intracrustal reflections that have been tentatively identified by *Eiken* [1991] on MCS records from the crest of the Mohns Ridge may correspond to reflections originating at the top of the low-density body. The apparent pinch and swell form of this body defines a series of spreading cells, the center of one cell being where the Bouguer anomaly is the widest. Each spreading cell has its own surficial expression, which may consist in one or more than one eruptive center, each center being characterized by highly magnetized material: the same source at depth may have many different surficial expression on the seafloor, but this cannot be solved by our data set.

Acknowledgments. The present work was supported by the Marine Geosciences Department of IFREMER, and a Ph.D. grant to one of us (C.R.) by the Ministère de la Recherche et de la Technologie, France. We acknowledge the master and crew of R/V *Jean Charcot* and R/V *Le Suroit* and Félix Avedik, chief scientist of the Mohns Ridge project. We also thank M. Sellevoll, for his kind cooperation for building up the project and his permission for showing the MCS sections in this paper; Ingi Olafsson and Bernt Roed, for their friendship and all the time they spent in search of seismic reflectors on the MCS records from the Mohns Ridge; Wolfgang Baltzer, chief scientist of R/V *Meteor* cruise 88/7-3, and Colin Devey for their permission to use and publish the description of the dredges they acquired at the Mohns Ridge. Isabelle Lecomte performed the tomographic inversion with support by a grant of IFREMER during her thesis research at the Institut de Physique du Globe in Strasbourg under the direction of Gérard Wittlinger. J.-C. Sempere provided the computer program for the three-dimensional inversion of the magnetic data. Discussions with H.D. Needham, J.-C. Sempere, Philippe Patriat, Thierry Juteau, Lindsay Parson, and Brigitte Smith helped in the development of the model presented here. Jean-Pierre Le Formal helped in the acquisition and the processing of the data.

REFERENCES

Chapman, M. E., Techniques for interpretation of geoid anomalies, *J. Geophys. Res., 84*, 3793-3801, 1979.

Chen, Y., and W.J. Morgan, Rift valley/no rift valley transition at mid-ocean ridges, *J. Geophys. Res., 95*, 17,571-17,581, 1990a.

Chen, Y., and W.J. Morgan, A nonlinear rheology model for mid-ocean ridge axis topography, *J. Geophys. Res.*, 95, 17,583-17,604, 1990b.

Claerbout, J.F., *Imaging the Earth's interior*, Blackwell Scientific, Boston, Mass., 398 pp., 1985.

Dauteuil, O., and J.P. Brun, Oblique rifting in a slow-spreading ridge, *Nature*, 361, 145-*148*, 1993.

Detrick, R. S., Ridge crest magma chambers: a review of results from recent marine seismic experiments, in Ophiolites-Genesis *and Evolution of the Oceanic Lithosphere*, edited by T. Peters, A. Nicolas, and R. Coleman, Kluwer Academic, Hingham, Mass., 1991

Detrick, R. S., J. C. Mutter, P. Buhl, and I. I. Kim, No evidence from multichannel reflection data for a crustal magma chamber in the MARK area on the Mid-Atlantic Ridge, *Nature, 347*, 61-64, 1990.

Eiken, O., Seismic-Reflection profiling along Mohns Ridge spreading ridge, Norwegian-Greenland Sea, *Seismo Ser., 59*, Inst. of Solid Earth Phys., Univ. of Bergen, Norway, 1991.

Fedhynskii, V. V., A. I. Rassokho, R. M. Demenitsikaya, A. M. Karasik, and S. S. Rozhdestvenskii, O strikture anomalhnogo magnitnogo polya yugo-zapadnoi chasti khrebta Mona, *Dokl. Akad. Nauk. SSSR, 223*, 726-729, 1975.

Fowler, C. M. R., and C. E. Keen, Oceanic crustal structure Mid-Atlantic Ridge at 45°N, *Geophys. J. R. Astron. Soc., 56*, 219-226, 1979.

Géli, L., Volcano-tectonic events and sedimentation since Late Miocene times at the Mohns Ridge, near 72°N, in the Norwegian Greenland Sea, *Tectonophysics, 222*, 417-444, 1993.

Gronlie, G., and M. Talwani, The free air gravity field of the Norwegian-Greenland Sea and adjacent areas, *Earth Evol.Sc., 2*, 74-103, 1982.

Heirtzler, J. R., and X. Le Pichon, The structure of mid-ocean ridges and magnetic anomalies over the Mid-Atlantic Ridge, *J. Geophys. Res., 70*, 4013-4033, 1965.

Hirschleber, H., F. Theilen, W. Balzer, B. Von Bodungen, and J. Thiede. Berichte au dem Sonderforschungsbereich 313 "Sedimentation im Europäischen Nordmeer", Forschungsschiff Meteor, Reise 7, vol. 1., Christian-Albrechts-Univ. zu Kiel, 1988.

Inoue, H., A least-squares smooth fitting for irregularly spaced data: Finite-element approach using the cubic B-spline basin, *Geophysics, 51*, 2051-2061, 1986.

Johnson, H. P., and T. M. Atwater, Magnetic study of basalts from the Mid-Atlantic Ridge, *Geol.* Soc. *Am. Bull., 88*, 637-647, 1977.

Kuo, B. Y., and D. W. Forsyth, Gravity anomalies of the ridge-transform system in the South Atlantic between 31 and 34,5°S: Upwelling centers and variations in crustal thickness, *Mar. Geophys. Res., 10*, 205-232, 1988.

Lecomte, I., Structure crustale d'une dorsale lente: Tomographie sismique 3D sur la dorsale de Mohn (72°20N, 1°30E), Ph.D. thesis, Univ. Louis Pasteur de Strasbourg, Strasbourg, France, 1990.

Lin, J., G. M. Purdy, H. Schouten, J. C. Sempéré, and C. Zervas, Evidence from gravity data for focused magmatic accretion along the Mid-Atlantic Ridge, *Nature, 344*, 627-632, 1990.

Macdonald, K.C., Mid-ocean ridges: Fine scale tectonic, volcanic and hydrothermal processes at the plate boundary zone, *Annu. Rev. Earth Planet. Sci., 10*, 155-190, 1982.

Macdonald, K.C., S. P. Miller, S. P. Huestis, and F. N. Spiess, Three-dimensional modeling of a magnetic reversal boundary from inversion of deep-tow measurements, *J. Geophys. Res., 85*, 3670-3680, 1980.

Neumann, E.-R., and J.G. Schilling, Petrology of basalts from the Mohns-Knipovich Ridge: The Norwegian-Greenland Sea, *Contrib. Mineral. Petrol., 85*, 204-233, 1984.

Olavsson I., L. Géli, and B.E. Roed, Multichannel seismic reflection profile across Mohns Ridge, Norwegian-Greenland Sea, *Seismo-Ser.*, Inst. of Solid Earth Phys., Univ. of Bergen, Norway, *20*, 1988.

Parker, R. L., and S. P. Huestis, The inversion of magnetic anomalies in the presence of topography, *J. Geophys. Res., 79*, 1587-1593, 1974.

Parsons, B., and J. G. Sclater, An analysis of the variation of ocean floor bathymetry and heat flow with age, *J. Geophys. Res., 82*, 803-827, 1977.

Patriat, P., Evolution du système de dorsale de l'océan Indien, Ph.D. thesis, Univ. Pierre et Marie Curie, Paris, France, 308 pp., 1985.

Perry, R. K., Bathymetry of the Nordic Seas, in *The Nordic Seas*, edited by B.G. Hurdle, pp. 211-236, Springer-Verlag, New York, 1986.

Prévot, M., A. Lecaille, and R. Hékinian, Magnetism of the Mid-Atlantic Ridge crest near 37°N from Famous and DSDP results: A review, in *Deep Drilling Results in the Atlantic Oceanic Crust*, edited by M. Talwani, C.G. Harrison, and D.E. Hayes, pp. 210-229, Maurice Ewing Ser., vol. 2, AGU, Washington, D.C., 1979.

Renard, V., F. Avedik, L. Géli, I. Lecomte, J.P. Le Formal, and A. Nercessian, Characterisitics of oceanic crust formation of a part of Mohns Ridge, near 72°N, in the Norwegian-Greenland Sea,. Part I, Morphological study and underway geophysics (abstract), *Terra Cognita, 1*, 207, 1989.

Roed, B., Geophysical investigations in the Mohns Ridge Area, Candidate Sci. thesis (in Norwegian), 89 pp., Seismol. Obs. Univ. of Bergen, Norway, 1989.

Rommevaux, C., C. Deplus, and P. Patriat, Thre-dimensional gravity study of the Mid-Atlantic Ridge: Evolution of the segmentation between 28° and 29°N during the last 10 m.y., *J. Geophys. Res.*, this issue.

Schouten, H., K.D. Klitgord, and J.A. Whitehead, Segmentation of mid-ocean ridges, *Nature, 317*, 225-229, 1985.

Searle, R. C., and A.S. Laugton, Fine scale sonar study of tectonics and volcanism on the Reykjanes Ridge, Oceanologica Acta, C4, 5-13, 1981.

Sempéré, J. C., G. M. Purdy, and H. Schouten, Segmentation of the Mid-Atlantic Ridge between 24°N and 30°40'N, *Nature, 344*, 427-431, 1990.

Sinton, J. M., and R. S. Detrick, Mid-ocean ridge magma chambers, *J. Geophys. Res.*, *97*, 197-216, 1992.

Sleep, N. H., Sensitivity of heat flow and gravity to the mechanism of seafloor spreading, *J. Geophys. Res.*, *74*, 542-549, 1969.

Talwani M., and O. Eldholm, Evolution of the Norwegian Greenland Sea, *Geol. Soc. Am. Bull.*, *88*, 969-999, 1977.

Talwani, M., J. Worzel, and M. Landisman, Rapid gravity computations for two-dimensional bodies with application to the Mendocino submarine fracture zone, *J. Geophys. Res.*, *64*, 49-59, 1959.

Talwani, M., C. C. Windisch, and M. G. Langseth, Reykjanes ridge crest: a detailed geophysical study, *J. Geophys. Res.*, *76*, 473-517, 1971.

Tapponnier, P., and J. Francheteau, Necking of the lithosphere and the mechanics of slowly accreting plate boundaries, *J. Geophys. Res.*, *83*, 3955-3970, 1978.

Toomey, D. R., S.C. Solomon, and G.M. Purdy, Microearthquakes beneath median valley of Mid-Atlantic Ridge near 23°N: Hypocenters and focal mechanisms, *J. Geophys. Res.*, *93*, 9093-9112, 1985.

Vogt, P. R., Geophysical and geochemical signatures and plate tectonics, in *The Nordic Seas*, edited by B.G. Hurdle, pp. 413-662, Springer-Verlag, New York, 1986.

Vogt, P. R., L. C. Kovacs, C. Bernero, and S. P. Srivastava, Asymmetric geophysical signatures in the Greenland-Norwegian and southern Labrador seas and the Eurasia Basin, *Tectonophysics*, *89*, 95-150, 1982.

Wessel, P., and A. B. Watts, On the accuracy of marine gravity measurements, *J. Geophys. Res.*, *93*, 393-413, 1988.

Whitmarsh, R. B., Median valley refraction line: Mid-Atlantic Ridge at 37°N, *Nature*, *246*, 297-299, 1973.

L. Géli and V. Renard, IFREMER, Département des Géosciences Marines, BP 70, 29280, Plouzané Cedex, France.

C. Rommevaux, Institut de Physique du Globe de Paris, Laboratoire de Géodynamique, 4, place Jussieu, 75252 Paris Cedex 05, France.

(Received December 14, 1992; revised October 13, 1993 ;
accepted October 21, 1993.)